Geosci. Model Dev. Discuss., https://doi.org/10.5194/gmd-2017-287
Manuscript under review for journal Geosci. Model Dev.
Discussion started: 5 December 2017


Geoscientific Model Development Discussions
Open Access
EGU

# A representation of the collisional ice break-up process in the two-moment microphysics scheme LIMA v1.0 of Meso-NH

Thomas Hoarau[1], Jean-Pierre Pinty[2], and Christelle Barthe[1]

[1]Laboratoire de l'Atmosphère et Cyclones, UMR 8105, CNRS/Météo-France/Université de La Réunion, St Denis, La Réunion, France
[2]Laboratoire d'Aérologie, University of Toulouse/CNRS/UPS, 14 avenue Edouard Belin, F-31400 Toulouse, France

*Correspondence to:* jean-pierre.pinty@aero.obs-mip.fr

**Abstract.** The paper describes a switchable parameterization of CIBU (Collisional Ice Break-Up), an ice multiplication process that fits in with the two-moment microphysical scheme LIMA (Liquid Ice Multiple Aerosols). The LIMA scheme with three ice types (pristine cloud ice crystals, snow-aggregates and graupel-hail) was developed in the cloud-resolving mesoscale model Meso-NH.

Here the CIBU process assumes that collisional break-up is mostly efficient for small snow-aggregate class of particles with a fragile structure when hit by large and dense graupel particles. The increase of cloud ice number concentration depends on a prescribed number of fragments being produced per collision. This point is discussed and analytical expressions of the newly contributing CIBU terms in LIMA are given.

The scheme is run in Meso-NH for the case of a three-dimension deep convective cloud with a heavy production of graupel. The consequence of dramatically changing the number of fragments produced per collision is explored in particular to estimate an upper bound of the CIBU effect. The case of a random number of fragments is also proposed to illustrate the consequence of the uncertainty of this parameter. Finally it is concluded that the assessment of CIBU certainly needs accurate laboratory experiments to check the conditions and to tune the efficiency of the process of ice crystal fragmentation. However the proposed parameterization which can be easily implemented in many two-moment microphysics schemes, could be used in this form to simulate the case of real deep tropical clouds where anomalously high concentrations of small ice crystals are suspected to occur.

Geosci. Model Dev. Discuss., https://doi.org/10.5194/gmd-2017-287
Manuscript under review for journal Geosci. Model Dev.
Discussion started: 5 December 2017


Geoscientific Model Development Discussions
Open Access
EGU

## 1 Introduction

In a series of paper, Yano and Phillips (2011, 2016) and Yano et al. (2016) brought the Collisional Ice Break-Up (hereafter CIBU) process to the fore again as a possible secondary ice production mechanism in clouds. Using an analytical model, they showed that the CIBU could lead to an explosive growth of small ice crystal concentrations. Afterwards Sullivan et al. (2017) tried to include CIBU in a parcel model of six species, assumed to be monodispersed here, in an attempt to make this finding specific. However intriguingly and in contrast to the Hallett-Mossop (hereafter H-M) ice multiplication mechanism[1] (Hallett and Mossop, 1974), the CIBU process was not perceived as a particulary important feature in cloud physics and is ignored in the vast majority of the currently used microphysics schemes. Yest, even without absolutely incontestable clues, still missing even in recently published cloud data records[2], the CIBU process is very likely to be active when cloud conditions are deemed favourable (Hobbs and Rangno, 1985; Rangno and Hobbs, 2001). For instance, collisions between large dense graupel growing by riming, and plane vapour-grown dendrites or irregular weakly rimed assemblages are the most conceivable scenario for generating multiple ice debris as envisioned by Hobbs and Farber (1972) and by Griggs and Choularton (1986). So a legitimate quest for a mixed-phase microphysics model such as LIMA (an acronym for Liquid, Ice, Multiple Aerosols, see Vié et al. (2016)) is to find ways to include an ice-ice break-up effect and to characterize its importance, relatively to other ice generating processes like ice heterogeneous nucleation, in the context of a two-moment scheme where number concentrations and mixing ratios of the ice crystals are predicted.

As recalled by Yano and Phillips (2011), the first few laboratory experiments dedicated to the study of ice collisions were conducted in the 1970s following investigations concerning the promising H-M process. The pioneering work of Vardiman (1978) was a rare experimental reference showing evidence for the mechanical fracturing of natural ice crystals. An interesting issue of the study was to show that the number of fragments was dependent on the shape of the initial colliding crystal and on the momentum change following the collision. According to a concluding remark of Vardiman (1978), this 'secondary' production of ice could lead to concentrations as high as 100 to 1000 times the expected natural concentrations of ice crystals in clouds from heterogeneous nucleation on ice freezing nuclei. Another laboratory study by Takahashi et al. (1995) also revealed a huge production of splinters after collisions between rimed and deposition-grown graupels. However the experimental set-up used there was more appropriate to very big, artificially grown crystals and to large impact velocities because as many as 400 fragments could be obtained.

For clarity, this study does not focus on cloud conditions leading to an explosive ice multiplication by mechanical break-up in ice-ice collisions (Yano and Phillips, 2011). Neither does it attempt to reformulate this process on the basis of collisional kinetic energy with many empirical parameters

[1] H-M is based on the explosive riming of "big" droplets on graupel particles in a narrow range of temperature
[2] An inventory of the secondary ice production mechanisms is given in Table 1 of Field et al. (2017)

Geosci. Model Dev. Discuss., https://doi.org/10.5194/gmd-2017-287
Manuscript under review for journal Geosci. Model Dev.
Discussion started: 5 December 2017


Geoscientific Model Development Discussions
Open Access
EGU

as proposed by Phillips et al. (2017), or earlier by Hobbs and Farber (1972) with the breaking energy, mostly for application to "bin" microphysics schemes. Here, the goal is rather to describe an empirical but realistic parameterization of CIBU to operate with several processes in microphysics (heterogeneous ice nucleation, cloud droplet freezing, H-M process, crystal aggregation) that shape the concentration of the small ice crystals in the well-suited LIMA scheme (Vié et al., 2016). Our idealization of CIBU is the formation of cloud ice crystals as the result of asymmetric collisions between big graupel particles and small aggregates followed by the erosion of the latter by the former. The parameterization of CIBU relies on the laboratory observations of Vardiman (1978) to set limits on the number of fragments per collision. However, the large uncertainties attached to this parameter encourage us to run exploratory experiments with several fixed values and also to model the number of fragments by means of a random process spanning two decades.

The LIMA scheme is inserted in Meso-NH (Lafore et al., 1998) for several sensitivity experiments to evaluate the importance of the CIBU process and the impact of the tuning i.e., the number of fragments produced per collision. The efficiency of CIBU to dramatically increase the concentration of small ice crystals can be scaled by the nucleation process yield. The case of a three-dimensional continental deep convective storm, the well-known STERAO case analysed by Skamarock et al. (2000), provided a framework for several adjustments of the number of ice fragments. A series of experiments was then performed for the same case to see how much the CIBU process altered the precipitation and the persistence of convective plumes. The question of the number of ice nuclei necessary to initate CIBU (Field et al., 2017) is also tackled. Finally a conclusion is drawn on the usefulness of systematically considering CIBU and other sources of ice multiplication in all mixed-phase two-moment schemes.

## 2 Introduction of CIBU into the LIMA scheme

### 2.1 General considerations

In contrast to the work of Yano and Phillips (2011) where large and small graupel particles fuelled the CIBU process, here we consider collisions involving two types of precipitating ice: small aggregates covering pristine ice crystals larger than $\sim$150 $\mu$m and large graupel particles. Shocks between graupel particles of different sizes are not considered because according to Griggs and Choularton (1986), the fragmentation of rime is very unlikely to occur in natural clouds. For the sake of simplicity and because the impact velocity of the graupel particles should be well above 1 m s$^{-1}$ to enter the break-up regime of the aggregates, the particle sizes are taken to stay within a range of substantial occurrence of CIBU.

A symbolic form of the equation describing the CIBU process can be written

$$\frac{\partial n_i}{\partial t} = \alpha n_s n_g \tag{1}$$

Geosci. Model Dev. Discuss., https://doi.org/10.5194/gmd-2017-287
Manuscript under review for journal Geosci. Model Dev.
Discussion started: 5 December 2017


Geoscientific Model Development Discussions
Open Access
EGU

where $n$ is the number concentration of the cloud ice (subscript "$i$"), the snow-aggregates ("$s$") and the graupel particles ("$g$"). $\alpha$ is the snow-aggregate-graupel collision kernel times $\mathcal{N}_{sg}$, the number of ice fragments produced by collision. The simplest expression of $\alpha$ is

$$\alpha = \mathcal{N}_{sg} V_{sg} \frac{\Pi}{4} D_g^2 \tag{2}$$

where $V_{sg}$ is the impact velocity of a graupel particle of size $D_g$ at the surface of the aggregate.

In Eq. 2, it is assumed that the size of the aggregate is negligible compared to $D_g$. $V_{sg}$ is expressed as the difference of fall speed between the colliding graupel and the aggregate target so $V_{sg} = (\rho_{00}/\rho_a)^{0.4} \times (c_g D_g^{d_g} - c_s D_s^{d_s})$ using the generic formula of the particle fall speeds $V_x = (\rho_{00}/\rho_a)^{0.4} \times c_x D_x^{d_x}$ with the air density correction of Foote and du Toit (1969) due to the drag force exerted by the particles during their fall. $\rho_{00}$ is the reference air density $\rho_a$ at normal pressure.

As introduced above and suggested in Yano and Phillips (2011), the impact velocity $V_{sg}$ should be such that a minimum value is guaranteed to enable CIBU. An easy way to do this is to restrict the size of the aggregates to the range [$D_{smin}$=0.2 mm, $D_{smax}$=1 mm] and to introduce a minimum size of $D_{gmin}$=2 mm for the graupel particles. The reasons for these choices are discussed the following. The lower bound value $D_{smin}$ is an estimate that results in the collision efficiency with a graupel particle approaching unity. For $D_s < D_{smin}$, big crystals or aggregates stay outside the path of capture which explains the observation of bimodal ice spectra. Field (2000) reported minimum values of 150-200 µm for $D_{trough}$, a critical size separating cloud ice and aggregate regimes. The $D_{smin}$ value is also consistent with an upper bound of the cloud ice crystal size distribution that results from the critical diameter of 125 µm to convert cloud ice to snow by deposition (see Harrington et al. (1995) for the original and analytical developments and Vié et al. (2016) for the implementation in LIMA). The choice of $D_{smax}$ and $D_{gmin}$ are dictated by the empirical rule that $V_{sg}$ >1 m s$^{-1}$. With the setup in LIMA which is $[c_x,\ d_x] = [5.1,\ 0.27]$ for "$x = s$" and $[124,\ 0.66]$ for "$x = g$" in MKS units, the least favourable situation gives $V_{sg}$=1.26 m s$^{-1}$ at ground level.

The number of fragments $\mathcal{N}_{sg}$ is the critical parameter for ice multiplication. From scaling arguments Yano and Phillips (2011) recommended taking $\mathcal{N}_{sg} = 50$. Recently Yano and Phillips (2016) introduced a notion of random fluctuations into the production of fragments leading to a stochastic equation of the ice crystal concentration due to the realization of a noise process for $\alpha$ (Eq. 2). The parameterization of $\mathcal{N}_{sg}$ as a function of collisional kinetic energy (Phillips et al., 2017) enables a differentiated treatment of the fragmentation of a variety of ice crystals. All these results start from Fig. 6 in Vardiman (1978) which suggests that $\mathcal{N}_{sg}$ is a function of momentum change, $\Delta M_g$, after the collision. As $\Delta M_g \sim 0.1$ g cms$^{-1}$ for $D_g$=2 mm, the corresponding $\mathcal{N}_{sg}$ lies between 10 (for collision with plane dendrites) and 40 (for rimed spatial crystals). These values are consistent with those found by Yano and Phillips (2011) for rimed assemblages. In conclusion, it is tempting to run both deterministic and stochastic simulations to test the sensitivity to $\mathcal{N}_{sg}$ but in the range suggested by laboratory experiments. In the following $\mathcal{N}_{sg}$ was set successively to 0.1 (weak effect) or alternatively one fragment per ten collisions, and 1.0 (moderate effect) and 10.0 (strong effect) fragments

Geosci. Model Dev. Discuss., https://doi.org/10.5194/gmd-2017-287
Manuscript under review for journal Geosci. Model Dev.
Discussion started: 5 December 2017


Geoscientific Model Development Discussions

per collision. Additional experiments were performed by first generating a random variable $X$ uniformly distributed over $[0.0,\ 1.0]$ and then by applying an empirical formula, $\mathcal{N}_{sg} = 10^{2.0\times X-1.0}$, to generate numbers over two decades $[0.1,\ 10.0]$ of $\mathcal{N}_{sg}$. The randomization of $\mathcal{N}_{sg}$ reflected the fact that the number of fragments depended on the positioning of the impact shock on the tip or on the body of the fragile particle and also on the energy used to cause the possible rotation of the residual particle.

### 2.2 Application to a 2-moment scheme

In a 2-moment scheme, the zeroth order (number concentration) and "xth" order (mixing ratio)[3] moments of the size distributions are computed. So from Eqs.1 and 2 with expansion, the CIBU tendency of the number concentration of the cloud ice $N_i$ (here in $\#\,\mathrm{kg}^{-1}$) can be written as:

$$\frac{\partial N_i}{\partial t} = \rho_{dref}\mathcal{N}_{sg}\frac{\Pi}{4}\left(\frac{\rho_{00}}{\rho_{dref}}\right)^{0.4}\int_{D_{smin}}^{D_{smax}} n_s(D_s)\left\{\int_{D_{gmin}}^{\infty} D_g^2(c_g D_g^{d_g} - c_s D_s^{d_s})n_g(D_g)\mathrm{d}D_g\right\}\mathrm{d}D_s \quad (3)$$

where $\rho_{dref}(z)$ is a reference density profile of dry air (Meso-NH is anelastic) and with a further approximation $\rho_a = \rho_{dref}$.

In LIMA, the size distributions follow a generalized gamma law:

$$n(D)\mathrm{d}D = N\frac{\alpha}{\Gamma(\nu)}\lambda^{\alpha\nu}D^{\alpha\nu-1}e^{-(\lambda D)^{\alpha}}\mathrm{d}D$$

where $\alpha$ and $\nu$ are fixed shape parameters, $N$ is the total number concentration and $\lambda$ is the slope parameter. With the definitions given in Appendix A, integration of Eq. 3 leads to:

$$\begin{aligned}\frac{\partial N_i}{\partial t} &= \rho_{dref}\mathcal{N}_{sg}\frac{\Pi}{4}\left(\frac{\rho_{00}}{\rho_{dref}}\right)^{0.4} N_s N_g \times \\ &\left\{c_g\left(M_s^{INC}(0;D_{smin}) - M_s^{INC}(0;D_{smax})\right)\left(M_g(2+d_g) - M_g^{INC}(2+d_g;D_{gmin})\right)\right. \\ &\left. - c_s\left(M_s^{INC}(d_s;D_{smin}) - M_s^{INC}(d_s;D_{smax})\right)\left(M_g(2) - M_g^{INC}(2;D_{gmin})\right)\right\} \quad (4)\end{aligned}$$

with $N_s = C_s\lambda_s^{x_s}$ and $N_g = C_g\lambda_g^{x_g}$. The set of flexible parameters used in LIMA is $C_s = 5,\ C_g = 5.\times 10^5,\ x_s = 1,\ x_g = -0.5$. These values were chosen to generalize the classical Marshall-Palmer law ($n(D) = N_0\ \exp(-\lambda D)$), a degenerate form of the generalized gamma law when $\alpha = \nu = 1$. It leads to a total concentration $N = N_0\lambda^{-1}$ with a fixed intercept parameter $N_0$.

Concerning the mixing ratios, the mass of the newly formed cloud ice fragments is simply taken as the product of the local mean mass of the pristine ice crystals by the $N_i$ tendency (Eq. 3). The mass of ice debris is equal to the mass loss of the aggregates after collisional break-up. The mass of

[3]Ice mixing ratios are computed by integration over the size distribution of the mass of individual particles given by a mass-size relationship (power law with a non-integer exponent "x")

Geosci. Model Dev. Discuss., https://doi.org/10.5194/gmd-2017-287
Manuscript under review for journal Geosci. Model Dev.
Discussion started: 5 December 2017


Geoscientific Model Development Discussions

the graupel is unchanged. The mass transfer from aggregates to small ice crystals is constrained by the mass of individual aggregates that may break up completely. This limiting mixing ratio tendency is given by:

$$\frac{\partial r_i}{\partial t} = -\frac{\partial r_s}{\partial t} = \frac{a_s}{\rho_{dref}} \frac{\Pi}{4} \left( \frac{\rho_{00}}{\rho_{dref}} \right)^{0.4} \int_{D_{smin}}^{D_{smax}} D_s^{b_s} n_s(D_s) \left\{ \int_{D_{gmin}}^{\infty} D_g^2 (c_g D_g^{d_g} - c_s D_s^{d_s}) n_g(D_g) \mathrm{d}D_g \right\} \mathrm{d}D_s. \tag{5}$$

In the above expression the mass of an aggregate of size $D_s$ is given by $a_s D_s^{b_s}$ with $a_s$=0.02 and $b_s$=1.9 in LIMA, meaning that aggregates are quasi two-dimensional particles. After integration the mixing ratio tendency is expressed as:

$$\begin{aligned} \frac{\partial r_i}{\partial t} = & \frac{a_s}{\rho_{dref}} \rho_{dref} \frac{\Pi}{4} \left( \frac{\rho_{00}}{\rho_{dref}} \right)^{0.4} N_s N_g \times \\ & \left\{ c_g \left( M_s^{INC}(b_s; D_{smin}) - M_s^{INC}(b_s; D_{smax}) \right) \left( M_g(2+d_g) - M_g^{INC}(2+d_g; D_{gmin}) \right) \right. \\ & \left. - c_s \left( M_s^{INC}(b_s+d_s; D_{smin}) - M_s^{INC}(b_s+d_s; D_{smax}) \right) \left( M_g(2) - M_g^{INC}(2; D_{gmin}) \right) \right\} \end{aligned} \tag{6}$$

This expression is independent of the number of fragments $\mathcal{N}_{sg}$.

## 3 Simulation of a 3-dimensional deep convective case

The test case is illustrated by idealized numerical simulations of the 10 July 1996 thunderstorm in the Stratospheric-Tropospheric Experiment: Radiation, Aerosols, and Ozone (STERAO) experiment. The simulations were initialized with the sounding given in Skamarock et al. (2000) and convection was triggered by three 3K-buoyant bubbles aligned along the main diagonal. Meso-NH was run for several hours over a domain of 320 × 320 gridpoints with 1 km-horizontal grid spacing. There were 50 unevenly spaced vertical levels up to 23 km height. With the exception of the wind component, all the fields including microphysics, were transported by an accurate, conservative, positive-definite PPM scheme (Colella and Woodward, 1984).

The aerosols were initialized as for the simulated squall-line case in Vié et al. (2016). A summary is given in Table 1 for the soluble Cloud Condensation Nuclei (CCN) and for the insoluble Ice Freezing Nuclei (IFN). Homogeneous vertical profiles are assumed for the aerosols. Although the LIMA scheme incorporates size distribution parameters and differentiates between the chemical compositions of the CCN and IFN, details regarding the characteristics of the five aerosol modes have no importance for the simulations shown here except for the sensitivity of CIBU to the initial concentration of the IFN which is explored at the end of the study.

Geosci. Model Dev. Discuss., https://doi.org/10.5194/gmd-2017-287
Manuscript under review for journal Geosci. Model Dev.
Discussion started: 5 December 2017


Geoscientific Model Development Discussions
Open Access
EGU

### 3.1 Impact on precipitation

Figure 1 shows the accumulated precipitation at ground level after 4 hours of simulation for the four experiments corresponding to $\mathcal{N}_{sg}$=0.0, 0.1, 1.0 and 10.0. The highest amount of rainfall is obtained when the CIBU process is ignored ($\mathcal{N}_{sg}$=0.0) in Fig. 1a. Then stepping up the CIBU efficiency by decade from $\mathcal{N}_{sg}$=0.1, Fig. 1b-d clearly shows a steady reduction of precipitation and a fine scale modification of the precipitation pattern. Furthermore, Fig. 1d reveals that the spread of the precipitation field, caused by the motion of the multicellular storm, is reduced significantly when $\mathcal{N}_{sg}$=10.0. The results of Fig. 1 suggest empirically that a plausible range for $\mathcal{N}_{sg}$ is between 0.1 and 10.0 fragments per collision. A value lower than 0.1 leads to a negligible effect of CIBU in the simulation, while taking $\mathcal{N}_{sg}$>10.0 produces an excessive (unrealistic) impact on the storm development (not shown). In complement, Fig 2 shows the results of a simulation, hereafter called "RANDOM", where $\mathcal{N}_{sg}$ is generated by a random process as explained above but providing $0.1 < \mathcal{N}_{sg} < 10.0$. The perturbation caused by CIBU is noticeable in this case too but it remains weak for the precipitation field. From these first 3D numerical experiments, it can be concluded that CIBU is clearly a disruptive process when $\mathcal{N}_{sg} > 10.0$ fragments per aggregate-graupel collision considering, the adverse impact on the precipitation field. Taking $0.1 < \mathcal{N}_{sg} < 10.0$ and, furthermore, taking $\mathcal{N}_{sg}$ as the realization of a random process, seems to be a more satisfactory approach. So the recommended upper bound value of $\mathcal{N}_{sg}$ is much lower than the former $N_0$ = 50, used with the notation of Yano and Phillips (2011) in their box model.

### 3.2 Changes in the microphysics

Basically, intensifying the CIBU process by increasing $\mathcal{N}_{sg}$ enhances the concentration of the cloud ice crystals to the detriment of the mass growth in the snow-aggregate category of precipitating ice as these particles are more fragmented when $\mathcal{N}_{sg}$ is increased. However a counteracting effect is possible because the partial mass sink of the snow-aggregate particles also slows down the flux of graupel particles, which form essentially by heavy riming and conversion of the snow-aggregates. This point is now examined by looking at the ice in the high levels of the STERAO cells. Figures 3-5 reproduce the 10 minute average of the mixing ratios $r_i$, $r_s$ and $r_g$ at 12 km height of the 4 experiments $\mathcal{N}_{sg}$=0.0, 0.1, 1.0 and 10.0 after 4 hours. The increase of the cloud ice mixing ratio with $\mathcal{N}_{sg}$ is clear in the area covered by the 0.2 $\mathrm{g\,kg^{-1}}$ isocontour in Fig. 3. Simultaneously, a slight decrease of $r_s$ indicating a slow erosion of the mass of the aggregates is visible in Fig. 4. The effect on the graupel (Fig. 5) is even smaller but appears clearly for the case $\mathcal{N}_{sg}$=10.0 where less graupel is found. A last illustration is provided by Fig. 6, showing the number concentration of cloud ice $N_i$ at a higher altitude of 15 km. Again, the increase of $N_i$ follows $\mathcal{N}_{sg}$ with an explosive multiplication of $N_i$ when $\mathcal{N}_{sg}$=10.0 ($N_i$ is well above 1000 crystals $\mathrm{kg^{-1}}$ of dry air in this case). Figure 7 summarizes the behaviour of $r_i$, $r_s$, $r_g$ at 12 km height, and of $N_i$ at 15 km height, for

Geosci. Model Dev. Discuss., https://doi.org/10.5194/gmd-2017-287
Manuscript under review for journal Geosci. Model Dev.
Discussion started: 5 December 2017


Geoscientific Model Development Discussions
Open Access
EGU

the "RANDOM" simulation. The results are those expected but, when comparingthese results with Figs 3-6, it is not possible to find microphysics anomalies equivalent to the case where CIBU is not accounted for so "RANDOM" is a full simulation scenario that is intermediate between $\mathcal{N}_{sg}$=1 and $\mathcal{N}_{sg}$=10.

The analysis of the STERAO simulations continues by looking at the vertical profiles of microphysics budgets. The profiles are 10 minute averages of the cloudy columns that contain at least $10^{-3}$ g kg$^{-1}$ of condensate at any level. The column selection is updated at each time step because of the evolution and motion of the storm. Figure 8 shows the mixing ratio profiles in three cases: $\mathcal{N}_{sg}$ = 0.0, "RANDOM" and $\mathcal{N}_{sg}$ = 10.0. A key feature that shows up in Fig. 8a-c is the increase of the $r_i$ peak value at 11 km altitude. This change is accompanied by a reduction of $r_s$ (more visible betweeen cases b) and c)) and of $r_g$. The result is a decrease of the rain mixing ratio $r_r$, which is mostly fed by the melting of graupel. The low value of the mean $r_r$ profile, compared to the mixing ratios of the ice phase above, is explained by the fact that rain is spread over fewer grid points than the ice in the anvil (the mixing ratio profiles are averaged over the same number of columns).

### 3.3 Budget of ice mixing ratios

The next step is dedicated to the microphysics tendencies (10 minute average again) of the ice mixing ratios in Fig. 9-11 to assess the impact of the CIBU process. We do not discuss the case of the liquid phase here because the tendencies (not shown) are not very much affected by CIBU.

As expected, the tendencies of $r_i$ (Fig. 9a-c) are the most affected by the CIBU process. The main processes, standing out in Fig. 9a when CIBU is not activated, are CEDS (Deposition-Sublimation), essentially a gain term and AGGS, the main loss of $r_i$ by aggregation with a rate of $0.5\ 10^{-3}$ g kg$^{-1}$ s$^{-1}$. The loss of $r_i$ by CFRZ makes a moderate contribution as some raindrops are present in the glaciated part of the storm. With $\mathcal{N}_{sg}$=RANDOM, the $r_i$ tendencies are amplified even with a modest contribution of $\sim 0.2\ 10^{-3}$ g kg$^{-1}$ s$^{-1}$ for CIBU itself. The growth of AGGS which doubles at 10 km height is caused by the increase in the SEDI term and the presence of CIBU. The CFRZ contribution is also increased. The last case, with $\mathcal{N}_{sg}$=10 (Fig. 9c) confirms the general increase of the rates except for CFRZ, interpreted here as a lack of raindrops.

The budget of the snow/aggregate mixing ratio in Fig. 10 contains many processes of equivalent importance in the range $\pm 0.05\ 10^{-3}$ g kg$^{-1}$ s$^{-1}$ but SEDS dominates negatively at $z = 11,000$ m and positively at $z$ = 7,000 m. The inclusion of CIBU (Fig. 10b-c) mostly leads to an increase of AGGS, the other processes remaining almost the same. Finally many processes contribute to the evolution of the graupel mixing ratio profiles (Fig. 11). The strongest loss is in the GMLT term that converts graupel into rain (up to $-0.3\ 10^{-3}$ g kg$^{-1}$ s$^{-1}$) while the contact freezing of the raindrops (CFRZ) reaches $0.15\ 10^{-3}$ g kg$^{-1}$ s$^{-1}$. The sedimentation term SEDG lies between $-0.3\ 10^{-3}$ g kg$^{-1}$ s$^{-1}$ (at $z$ = 10,000 m) and $0.15\ 10^{-3}$ g kg$^{-1}$ s$^{-1}$ at 5,000 m). Another noticeable effect is the sign change of DEPG ($\pm 0.07\ 10^{-3}$ g kg$^{-1}$ s$^{-1}$) showing that the water vapour is

Geosci. Model Dev. Discuss., https://doi.org/10.5194/gmd-2017-287
Manuscript under review for journal Geosci. Model Dev.
Discussion started: 5 December 2017


Geoscientific Model Development Discussions
Open Access
EGU

super(under)saturated above(below) $z$=7,000 m on average. The relative importance of these processes does not change very much when CIBU is increased but tendencies weaken. In summary, the impact of CIBU is modest for the microphysics mixing ratios. The increase of ice fragments in $r_i$ is approximately compensated by an increase of AGGS (see Fig. 9 and 10).

### 3.4 Budget of cloud ice concentration

The next point examined is the behaviour of the cloud ice number concentration according to the strength of the CIBU process after 4 hours of simulation. Figure 12 shows that the altitude of the $N_i$ peak value decreases when $\mathcal{N}_{sg}$ increases. In the absence of CIBU ($\mathcal{N}_{sg}$ = 0), the origin of $N_i$ is the heterogeneous nucleation processes on insoluble IFN and coated IFN (nucleation by immersion) which are more efficient at low temperature. They provide a mean peak value $N_i$ = 400 $\mathrm{kg}^{-1}$ at $z$ = 11,500 m. In contrast, the $\mathcal{N}_{sg}$ = 10 case (here scaled by $\times 0.1$ for plotting reasons) keeps the trace of an explosive production of cloud ice concentration, $N_i$ = 7,250 $\mathrm{kg}^{-1}$, due to CIBU. The altitude of the maximum of $N_i$ in this case ($z$ = 10,000 m) is consistent with the location of the maximum value of the $r_s \times r_g$ product (see Fig. 8). The "RANDOM" simulation produces $N_i$ = 1100 $\mathrm{kg}^{-1}$ at $z$ = 11,000 m, a number concentration that is an order of magnitude lower. Table 2 reports the peak amplitude of the $N_i$ profiles as a function of $\mathcal{N}_{sg}$ but after 3 hours of simulation when the CIBU rate is strongly dominant. Additional cases were run to cover 0.1<$\mathcal{N}_{sg}$<50 with a logarithmic progression above $\mathcal{N}_{sg}$ = 1.0. The CIBU enhancement factor, $\mathrm{CIBU_{ef}}$, is computed as $N_i(\mathcal{N}_{sg})/N_i(\mathcal{N}_{sg}=0)-1$ as $N_i(\mathcal{N}_{sg})$ = 0 stands as a baseline that is not affected by the CIBU process. The results clearly show that the growth of $N_i$ is exponential as soon as $\mathcal{N}_{sg}$ reaches ∼5.0 ($\mathrm{CIBU_{ef}}$ switches from 135% to 913% when $\mathcal{N}_{sg}$ moves from 2.0 to 5.0). Taking $\mathcal{N}_{sg}$ = 50 leads to an enormous and definitely unrealistic value of the $N_i$ peak value.

The $N_i$ tendencies are the subject of Fig. 13. Many processes are involved during the temporal integration of $N_i$. The $\mathcal{N}_{sg}$ = 0 case confirms the importance of the heterogeneous nucleation process by deposition, HIND, (refer to Table 3) and to a lesser degree by immersion (HINC) at 8 km height. HIND peaks at three altitudes with two sources of IFN (Table 1). This case also reveals the importance of the HMG (1.3 $\mathrm{kg}^{-1}\mathrm{s}^{-1}$) and HMS (0.85 $\mathrm{kg}^{-1}\mathrm{s}^{-1}$) processes. Here, we consider that H-M also operates for the snow-aggregates because this category of ice is prone to light riming, like the graupel particles, in the case of water supercooling. These processes are first compensated by AGGS (capture of cloud ice by the aggregates). There is also a loss of cloud ice due to CFRZ and CEDS with the full sublimation of individual cloud ice crystals that replenish the IFN reservoir. The sedimentation profile transports ice from cloud top (SEDI<0) to mid-level cloud (SEDI>0). Then taking $\mathcal{N}_{sg}$ = RANDOM shows the domination of the CIBU process, which reaches 2.5 $\mathrm{kg}^{-1}\mathrm{s}^{-1}$ at 5 km height. The enhancement of HIND at cloud top can also be noted. The CIBU source of ice crystals is equilibrated by an increase of AGGS and, above all, of CEDS. Finally, the $\mathcal{N}_{sg}$ = 10 case

Geosci. Model Dev. Discuss., https://doi.org/10.5194/gmd-2017-287
Manuscript under review for journal Geosci. Model Dev.
Discussion started: 5 December 2017


Geoscientific Model Development Discussions
Open Access
EGU

290 demonstrates the reality of the exponential growth of $N_i$ because the three main driving terms CIBU, CEDS and AGGS are multiplied by a factor of approximately 5.

### 3.5 Sensitivity to the initial concentration of freezing nuclei

The purpose of the last series of experiments was to look more closely at the sensitivity of the cloud ice concentration to IFN initial concentration. Numerical simulations were run with $N_{IFN}$ 295 decreasing by decades from 100 dm$^{-3}$ to 0.001 dm$^{-3}$ for each IFN mode (see Table 1). Two different cases were considered. In the first one, CIBU was activated with the RANDOM set-up while, in the second, CIBU effects were ignored. All the results are summarized in the plots of Fig. 14.

Figure 14a shows that $N_i$ concentrations did not change very much for a wide range of initial $N_{IFN}$ concentrations, which were scanned by decades. This clearly illustrates the predominance 300 of the CIBU effect for current IFN concentrations, which disconnects $N_i$ concentrations from the underlying abundance of IFN particles. In this vein, the small hump superimposed on all profiles at 5,000 m height reveals a residual effect of the Hallett-Mossop process. A remarkable feature is also that a fairly low IFN concentration ($N_{IFN}$ = 0.001 dm$^{-3}$) suffices to initiate the CIBU process and to reach $N_i \sim 500$ kg$^{-1}$. In contrast and in the absence of CIBU (Fig. 14b), the $N_i$ profiles show a 305 sensitivity to IFN nucleation that is, indeed, difficult to interpret because of the non-monotonic trend of the $N_i$ profiles. Some insight can be gained from checking the concentration of the nucleated IFN of the first IFN mode (dust particles). In Fig. 14c, the IFN profiles are rescaled (multiplication by an appropriate numbers of powers of ten) to be comparable. The important result here is that the nucleated IFN evolve in close proportion to the initially available IFN concentrations, meaning 310 that the nucleating properties of the IFN do not depend on the IFN concentration as expected. The last plot (Fig. 14d) reproduces the normalized differences of $N_i$ profiles between simulations with CIBU and without CIBU. Even if twin simulations i.e., performed with the same initial $N_{IFN}$, may diverge because of additional non-linear effects (vertical transport, cloud ice sink processes), the figure gives a flavour of the bulk CIBU effect on $N_i$ concentrations. The enhancement ratio due to 315 CIBU remains low (less than 1 for $N_{IFN} \sim 100$ dm$^{-3}$) but can reach a factor of 20 at 9,000 m height in cases of initially moderate $N_{IFN}$ concentrations i.e. $N_{IFN} \sim 1$ dm$^{-3}$. The behaviour of LIMA can be explained in the sense that increasing $N_{IFN}$ too much leads to smaller pristine crystals that need a long time to grow because the conversion into the next category of snow-aggregates is size-dependent (see Harrington et al. (1995) and Vié et al. (2016)). On the other hand, a low 320 concentration of $N_{IFN}$ initiates fewer snow-aggregate particles and thus less graupel, so the whole CIBU efficiency is reduced. Thus, this study confirms the essential role of CIBU to compensate for IFN deficit when cloud ice concentrations are building up.

Geosci. Model Dev. Discuss., https://doi.org/10.5194/gmd-2017-287
Manuscript under review for journal Geosci. Model Dev.
Discussion started: 5 December 2017




## 4 Summary and perspectives

The aim of this work was to study a comprehensive parametrization of the Collisional Ice Break-Up for a bulk 2-moment microphysics scheme running in a cloud resolving mesoscale model (MesoNH in our case). While the process is suspected to occur in real clouds, it is not included in current bulk microphysics schemes. Because of uncertainties, the present parameterization has been kept as simple as possible. It considers only shocks between small aggregates and large dense graupel particles. The number of fragments $\mathcal{N}_{sg}$ is a key parameter but is still largely unknown. A merit of this study is that it gives arguments to empirically support limiting the value of $\mathcal{N}_{sg}$ to 10. Furthermore, we suggest considering $\mathcal{N}_{sg}$ as the realization of a random process because delicate radiating crystals undergoing fragmentation lead to crystals with a missing arm or to many irregular fragments as illustrated and discussed by Hobbs and Farber (1972). As a result it has been shown, for instance, that running with $\mathcal{N}_{sg} > 10$ in the STERAO deep convection test case, dramatically alters the precipitation at the ground because the conversion of cloud ice crystals into precipitating ice is slowed down. Simultaneously, a major expected effect of CIBU is clearly to increase the number concentration of small ice crystals.

The microphysics perturbation due to the activation of CIBU has been studied by looking at the profiles of mixing ratios, ice concentrations and corresponding budget terms. In particular, the CIBU effect on the pristine ice and aggregate mixing ratios is compensated by an enhancement of the capture of the small crystals by the aggregates. The sensitivity of the ice concentration to $\mathcal{N}_{sg}$ is demonstrated with a mean multplication factor as high as 25 for $\mathcal{N}_{sg}$ = 10. The last study on the sensitivity of the simulations to the initial IFN concentration showed that CIBU was mostly efficient for current IFN concentrations of $\sim$1 dm$^{-3}$. Furthermore the CIBU process was still active for very low IFN concentrations, down to 0.001 dm$^{-3}$, which were sufficient to initiate the ice phase.

The proposed parameterization is very easy to implement and to evaluate in other microphysics schemes where the growth of precipitating ice is represented differently. The tuning of the scheme can be revised as soon as laboratory experiments are available for more precise fixing of the sizes and the shapes of the crystals that may break following shocks and to estimate the variety of fragment numbers more accurately. As microphysics schemes are now used to produce quantitative precipitation forecasts, it is also imperative that the production of rain is not altered too much by an overstimation of the CIBU effect.

With new imagers, counters and improvements in data analysis (Ladino et al., 2017), more and more evidence is being presented that ice multiplication production is a dominant process in natural cloud. However, the explanation of anomalously high ice concentrations is difficult to link to a precise process (Rangno and Hobbs, 2001; Field et al., 2017). So the next step will consist of the LIMA scheme to introduce the shattering of raindrops during freezing as proposed by Lawson et al. (2017) and an analysis of its behaviour compared to CIBU, because the basic ingredients leading to the ice multiplication process are not the same. Then, the final task will be to check that microphysics

Geosci. Model Dev. Discuss., https://doi.org/10.5194/gmd-2017-287
Manuscript under review for journal Geosci. Model Dev.
Discussion started: 5 December 2017




schemes with all sources of small ice crystals are able to reproduce observed ice concentrations which can reach very high values (units of $cm^{-3}$) in deep clouds but for which no convincing explanations have yet been found.

## 5 Code availability

The Meso-NH code is publicly available at http://mesonh.aero.obs-mip.fr/mesonh51. Here the model development and the simulations were made with version "MASDEV5-1 BUG2". The modifications brought to the LIMA scheme (v1.0) are available upon request from Jean-Pierre Pinty and next in the Supplement related to this article and available at http://doi.org/10.5281/zenodo.1078527.

## Appendix A: Moments of the gamma and incomplete gamma functions

The $p^{th}$ moment of the generalized gamma function (see definition in the text) is

$$M(p) = \int_0^\infty D^p n(D) \mathrm{d}D = \frac{\Gamma(\nu + p/\alpha)}{\Gamma(\nu)} \frac{1}{\lambda^p} \tag{A1}$$

where the gamma function is defined as:

$$\Gamma(x) = \int_0^\infty t^{x-1} e^{-t} \mathrm{d}t. \tag{A2}$$

The $p^{th}$ moment of the incomplete gamma function is written

$$M^{INC}(p;X) = \int_0^X D^p n(D) \mathrm{d}D. \tag{A3}$$

The algorithm of the "GAMMA_INC$(p;X)$" function (Press et al., 1992) is used to tabulate $M^{IN}(p;X) \times \Gamma(p)$ (the "GAMMA" function of Press et al. (1992) is also used). A change of variable is necessary to take the generalized form of the gamma size distributions into account. As a result, $M^{INC}(p;X)$ is written:

$$M^{INC}(p;X) = M(p) \times \text{GAMMA\_INC}(\nu + p/\alpha; (\lambda X)^\alpha) \tag{A4}$$

with $M(p)$ given by Eq. A1.

*Acknowledgements.* J.-P. Pinty wishes to thank V. Phillips for discussions about his original work on the topic. This work was done during the PhD of T. Hoarau who is financially supported by Reunion Island Regional Council and the European Union Council. T. Hoarau thanks University of La Réunion for supporting a short stay at Laboratoire d'Aérologie. Mrs Susan Becker corrected the English of the manuscript. Preliminary computations were performed on the 36 node home-made cluster of Lab. Aérologie. J.-P. Pinty acknowledges CALMIP

Geosci. Model Dev. Discuss., https://doi.org/10.5194/gmd-2017-287
Manuscript under review for journal Geosci. Model Dev.
Discussion started: 5 December 2017




(CALcul MIdi-Pyrénés) of the University of Toulouse for access to the "Eos" supercomputer where useful additional simulations were performed. T. Hoarau and C. Barthe acknowledge the GENCI ressources for access to the "Occigen" supercomputer.

Geosci. Model Dev. Discuss., https://doi.org/10.5194/gmd-2017-287
Manuscript under review for journal Geosci. Model Dev.
Discussion started: 5 December 2017


Geoscientific Model Development Discussions
Open Access
EGU

## References

Colella, P. and Woodward, P.: The piecewise parabolic method (PPM) for gas-dynamical simulations, J. Comput. Phys., 54, 174–201, 1984.

Field, P. R.: Bimodal ice spectra in frontal clouds, Quart. J. Roy. Meteor. Soc., 126, 379–392, doi:10.1002/qj.49712656302, 2000.

Field, P. R., Lawson, R. P., Brown, P. R. A., Lloyd, G., Westbrook, C., Moisseev, D., Miltenberger, A., Nenes, A., Blyth, A., Choularton, T., Connolly, P., Buehl, J., Crosier, J., Cui, Z., Dearden, C., DeMott, P., Flossmann, A., Heymsfield, A., Huang, Y., Kalesse, H., Kanji, Z. A., Korolev, A., Kirchgaessner, A., Lasher-Trapp, S., Leisner, T., McFarquhar, G., Phillips, V., Stith, J., and Sullivan, S.: Secondary ice production: current state of the science and recommendations for the future, Meteor. Monogr., 58, 7.1–7.20, doi:10.1029/AMSMONOGRAPHS-D-16-0014.1, 2017.

Foote, G. B. and du Toit, P. S.: Terminal velocity of raindrops, J. Appl. Meteor., 8, 249–253, 1969.

Griggs, D. G. and Choularton, T. W.: A laboratory study of secondary ice article production by the fragmentation of rime and vapour-grown ice crystals, Quart. J. Roy. Meteor. Soc., 112, 149–163, doi:10.1002/qj.49711247109, 1986.

Hallett, J. and Mossop, S. C.: Production of secondary ice particles during the riming process, Nature, 249, 26–28, doi:10.1038/249026a0, 1974.

Harrington, J. Y., Meyers, M. P., Walko, R. L., and Cotton, W. R.: Parameterization of Ice Crystal Conversion Processes Due to Vapor Deposition for Mesoscale Models Using Double-Moment Basis Functions. Part I: Basic Formulation and Parcel Model Results, J. Atmos. Sci., 52, 4344–4366, doi:10.1175/1520-0469(1995)052<4344:POICCP>2.0.CO;2, 1995.

Hobbs, P. V. and Farber, R. J.: Fragmentation of ice particles in clouds, J. Rech. Atmos., 6, 245–258, 1972.

Hobbs, P. V. and Rangno, A. L.: Ice particle concentrations in clouds, J. Atmos. Sci., 42, 2523–2549, 1985.

Ladino, L. A., Korolev, A., Heckman, I., Wolde, M., Fridlind, A. M., and Ackerman, A. S.: On the role of ice-nucleating aerosol in the formation of ice particles in tropical mesoscale convective systems, Geophys. Res. Lett., 44, doi:10.1002/2016GL072 455, 2017.

Lafore, J. P., Stein, J., Asencio, N., Bougeault, P., Ducrocq, V., Duron, J., Fischer, C., Héreil, P., Mascart, P., Masson, V., Pinty, J.-P., Redelsperger, J.-L., Richard, E., and Vila-Guerau de Arellano, J.: The Meso-NH atmospheric simulation system. Part I: adiabatic formulation and control simulations, Annales Geophysicae, 16, 90–109, doi:10.1007/s00585-997-0090-6, 1998.

Lawson, R. P., Gurganus, C., Woods, S., and Bruintjes, R.: Aircraft observations of cumulus microphysics ranging from the Tropics to Midlatitudes: Implications for a "new" secondary ice process, J. Atmos. Sci., 74, 2899–2920, doi:10.1175/JAS-D-17-0033.1, 2017.

Phillips, V. T., Yano, J.-I., and Khain, A.: Ice multiplication by break-up in ice-ice collisions. Part I: Theoretical formulation, J. Atmos. Sci., 74, 1705–1719, doi:10.1175/JAS-D-16-0224.1, 2017.

Press, W. H., Teukolsky, S. A., Vetterling, W. T., and Flannery, B. P.: Numerical Recipes in FORTRAN: The Art of Scientific Computing, Cambridge University Press, New-York, 1992.

Rangno, A. L. and Hobbs, P. V.: Ice particles in stratiform clouds in the Arctic and possible mechanisms for the production of high ice concentrations, J. Geophys. Res., 106, 15 065–15 075, 2001.

Geosci. Model Dev. Discuss., https://doi.org/10.5194/gmd-2017-287
Manuscript under review for journal Geosci. Model Dev.
Discussion started: 5 December 2017




Skamarock, W. C., Powers, J. G., Barth, M., Dye, J. E., Matejka, T., Bartels, D., Baumann, K., Stith, J., Parrish, D. D., and Hubler, G.: Numerical simulations of the July 10 Stratospheric-Tropospheric Experiment: Radiation, Aerosol, and Ozone/Deep Convection Experiment convective system: Kinematics and transport, J. Geophys. Res., 105, 19,973–19,990, 2000.

Sullivan, S. C., Hoose, C., and Nenes, A.: Investigating the contribution of secondary ice production to in-cloud ice crystal numbers, J. Geophys. Res., 122, doi:10.1002/2017JD026 546, 2017.

Takahashi, T., Nagao, Y., and Kushiyama, Y.: Possible high ice particle productionduring graupel-graupel collisions, J. Atmos. Sci., 52, 4523–4527, 1995.

Vardiman, L.: The generation of secondary ice particles in clouds by crystal–crystal collision, Journal of the Atmospheric Sciences, 35, 2168–2180, doi:1520-0469(1978)035<2168:TGOSIP>2.0.CO;2, 1978.

Vié, B., Pinty, J.-P., Berthet, S., and Leriche, M.: LIMA (v1.0): A quasi two-moment microphysical scheme driven by a multimodal population of cloud condensation and ice freezing nuclei, Geoscientific Model Development, 9, 567–586, doi:10.5194/gmd-9-567-2016, 2016.

Yano, J.-I. and Phillips, V. T.: Ice–Ice Collisions: An Ice Multiplication Process in Atmospheric Clouds, J. Atmos. Sci., 68, 322–333, doi:10.1175/2010JAS3607.1, 2011.

Yano, J.-I. and Phillips, V. T.: Explosive Ice Multiplication Induced by multiplicative-Noise fluctuation of Mechanical Break-up in Ice-Ice Collisions, J. Atmos. Sci., 73, 4685–4697, doi:10.1175/JAS-D-16-0051.1, 2016.

Yano, J.-I., Phillips, V. T., and Kanawade, V.: Explosive ice multiplication by mechanical break-up in ice–ice collisions: a dynamical system-based study, Quart. J. Roy. Meteor. Soc., 142, 867–879, doi:10.1002/qj.2687, 2016.

Geosci. Model Dev. Discuss., https://doi.org/10.5194/gmd-2017-287
Manuscript under review for journal Geosci. Model Dev.
Discussion started: 5 December 2017


Geoscientific Model Development Discussions
Open Access
EGU

| CCN | Aitken mode | Accumulation mode | Coarse mode |
|---|---|---|---|
| $N$ ($\mathrm{cm}^{-3}$) | 300 | 140 | 50 |
| $d_X$ (µm) | 0.23 | 0.8 | 2.0 |
| $\sigma_X$ | 2.0 | 1.5 | 1.6 |

| IFN | Dust mode | BC+Organics mode |
|---|---|---|
| $N$ ($\mathrm{dm}^{-3}$) | 10 | 10 |
| $d_X$ (µm) | 0.8 | 0.2 |
| $\sigma_X$ | 2.0 | 1.6 |

**Table 1.** Background CCN and IFN configuration for the STERAO idealized case simulations.

Geosci. Model Dev. Discuss., https://doi.org/10.5194/gmd-2017-287
Manuscript under review for journal Geosci. Model Dev.
Discussion started: 5 December 2017


Geoscientific Model Development Discussions
Open Access
EGU

| $\mathcal{N}_{sg}$ (no unit) | 0.0 | 0.1 | 1.0 | 2.0 | 5.0 | 10.0 | 20.0 | 50 |
|---|---|---|---|---|---|---|---|---|
| $N_i$ ($\#\mathrm{kg}^{-1}$) | 790 | 940 | 1,160 | 1,860 | 8,000 | 25,670 | 62,010 | 112,740 |
| $\mathrm{CIBU}_{\mathrm{ef}}$ (%) | 0 | 19 | 47 | 135 | 913 | 3149 | 7749 | 14171 |

**Table 2.** After 3 hours of simulation, maximum value of the cloud ice number concentration $N_{i_{max}}$ as a function of the number of fragments produced per snow/aggregate-graupel collision $\mathcal{N}_{sg}$. The last row is the CIBU enhancement factor $\mathrm{CIBU}_{\mathrm{ef}}$ in percent (see text).

Geosci. Model Dev. Discuss., https://doi.org/10.5194/gmd-2017-287
Manuscript under review for journal Geosci. Model Dev.
Discussion started: 5 December 2017


Geoscientific Model Development Discussions

| Process Acronym | Description |
|---|---|
| ACC | Raindrop accretion on snow to produce graupel |
| AGGS | Snow growth by capture of cloud ice |
| BERFI | Growth of cloud ice by Bergeron-Findeisen process |
| CEDS | Deposition/sublimation of water vapour on cloud ice |
| CFRZ | Raindrop Freezing by contact with cloud ice |
| CIBU | Snow break-up by collision with graupel |
| CMEL | Conversion Melting of snow into graupel |
| CNVI | Decreasing snow converted back to cloud ice |
| CNVS | Growing cloud ice converted into snow |
| DEPG | Water vapour deposition on graupel |
| DEPS | Water vapour deposition on snow |
| DRYG | Graupel dry growth (water can freeze fully) |
| HINC | Heterogeneous nucleation by immersion |
| HIND | Heterogeneous nucleation by deposition |
| HONC | Homogeneous freezing of the cloud droplets |
| HONH | Haze homogeneous freezing |
| HMG | Droplet riming and Hallett-Mossop process on graupel |
| HMS | Droplet riming and Hallett-Mossop process on snow |
| HMS | Water vapour deposition on snow |
| IMLT | Melting of cloud ice |
| RIM | Riming of cloud droplets on snow to produce graupel |
| SEDI | Sedimentation of cloud ice, snow or graupel |
| WETG | Graupel wet growth (water is partially frozen) |

**Table 3.** Nomenclature of the microphysics processes of the budget profiles.

Geosci. Model Dev. Discuss., https://doi.org/10.5194/gmd-2017-287
Manuscript under review for journal Geosci. Model Dev.
Discussion started: 5 December 2017


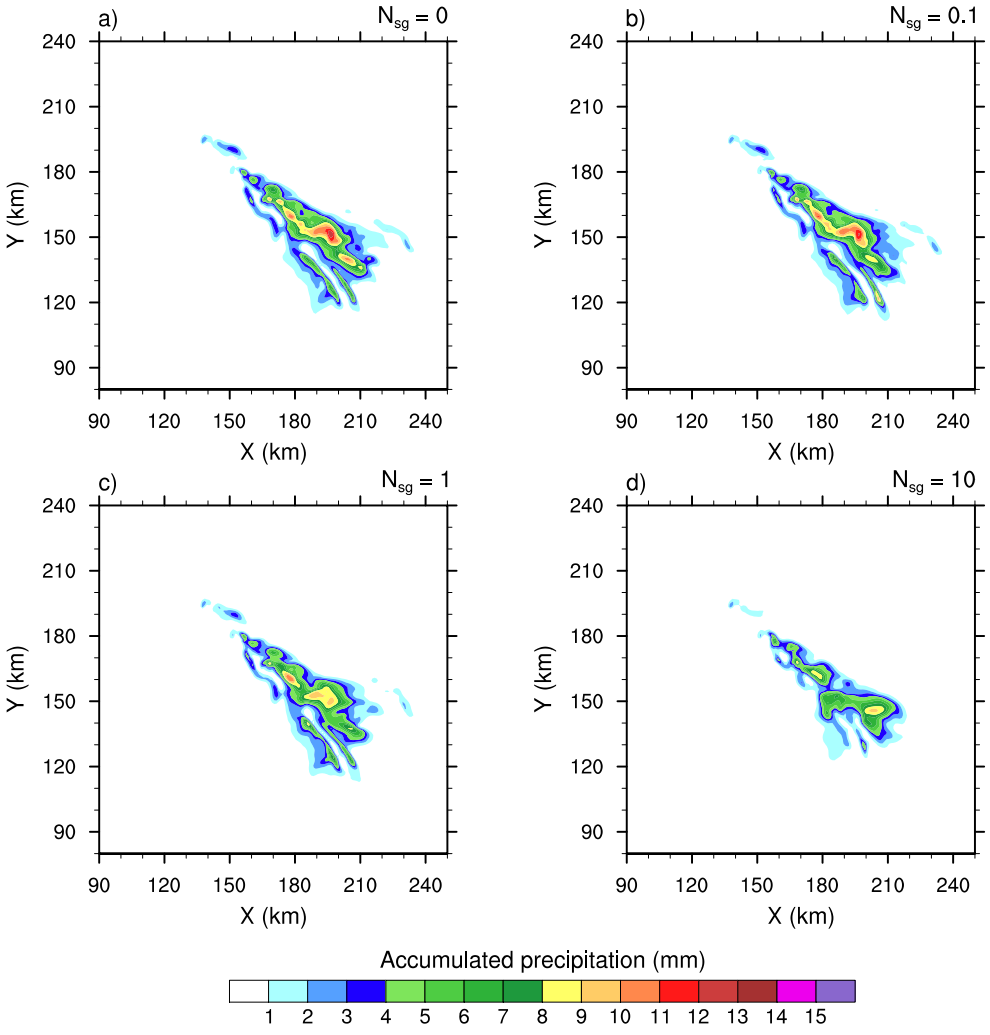


**Figure 1.** 4-h accumulated precipitation of the STERAO simulations where a) to d) refers to cases with $\mathcal{N}_{sg}$=0.0, 0.1, 1.0 and 10.0 ice fragments per collision, respectively. The plots are for a fraction of the computational domain.

Geosci. Model Dev. Discuss., https://doi.org/10.5194/gmd-2017-287
Manuscript under review for journal Geosci. Model Dev.
Discussion started: 5 December 2017


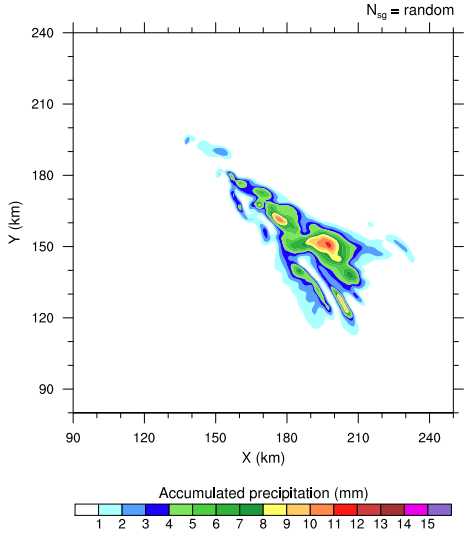


**Figure 2.** Same as Fig. 1, but for the "RANDOM" simulation.

Geosci. Model Dev. Discuss., https://doi.org/10.5194/gmd-2017-287
Manuscript under review for journal Geosci. Model Dev.
Discussion started: 5 December 2017


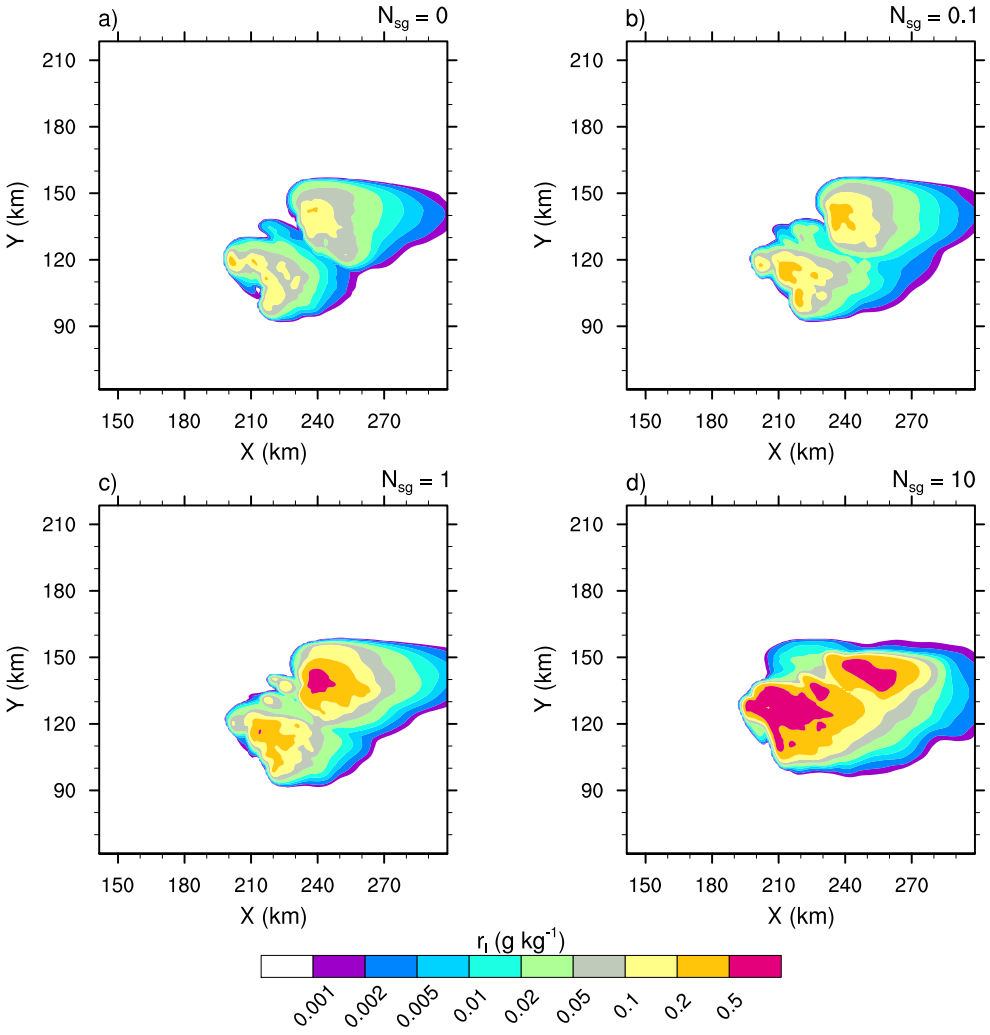


**Figure 3.** Mixing ratios of the cloud ice ($r_i$ in log scale) of the STERAO simulations at 12 km height, where a) to d) refer to cases with $\mathcal{N}_{sg}$=0.0, 0.1, 1.0 and 10.0 ice fragments per collision, respectively. The plots are for a fraction of the computational domain.

Geosci. Model Dev. Discuss., https://doi.org/10.5194/gmd-2017-287
Manuscript under review for journal Geosci. Model Dev.
Discussion started: 5 December 2017


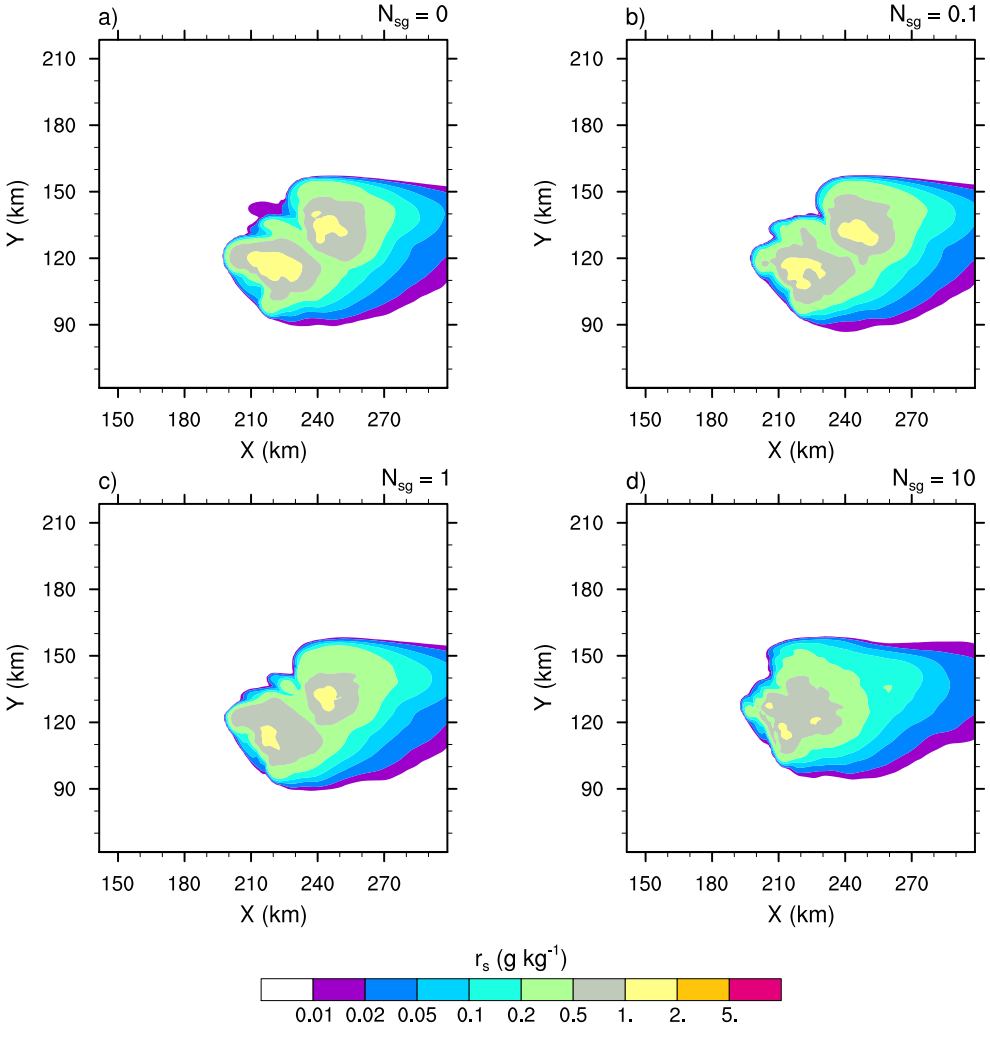


**Figure 4.** Same as Fig. 3 but for the mixing ratios of snow-aggregates ($r_s$).

Geosci. Model Dev. Discuss., https://doi.org/10.5194/gmd-2017-287
Manuscript under review for journal Geosci. Model Dev.
Discussion started: 5 December 2017


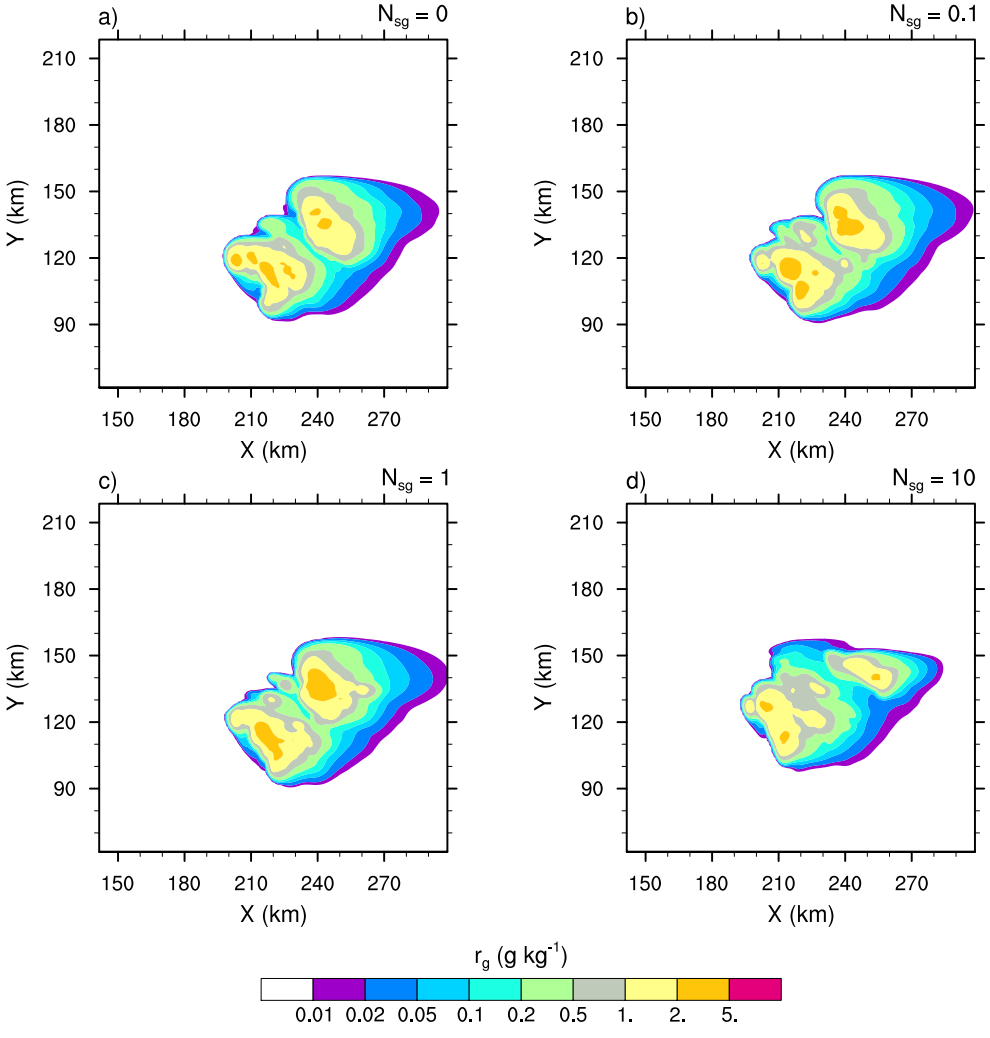


**Figure 5.** Same as Fig. 3 but for the mixing ratios of graupel ($r_g$).

Geosci. Model Dev. Discuss., https://doi.org/10.5194/gmd-2017-287
Manuscript under review for journal Geosci. Model Dev.
Discussion started: 5 December 2017


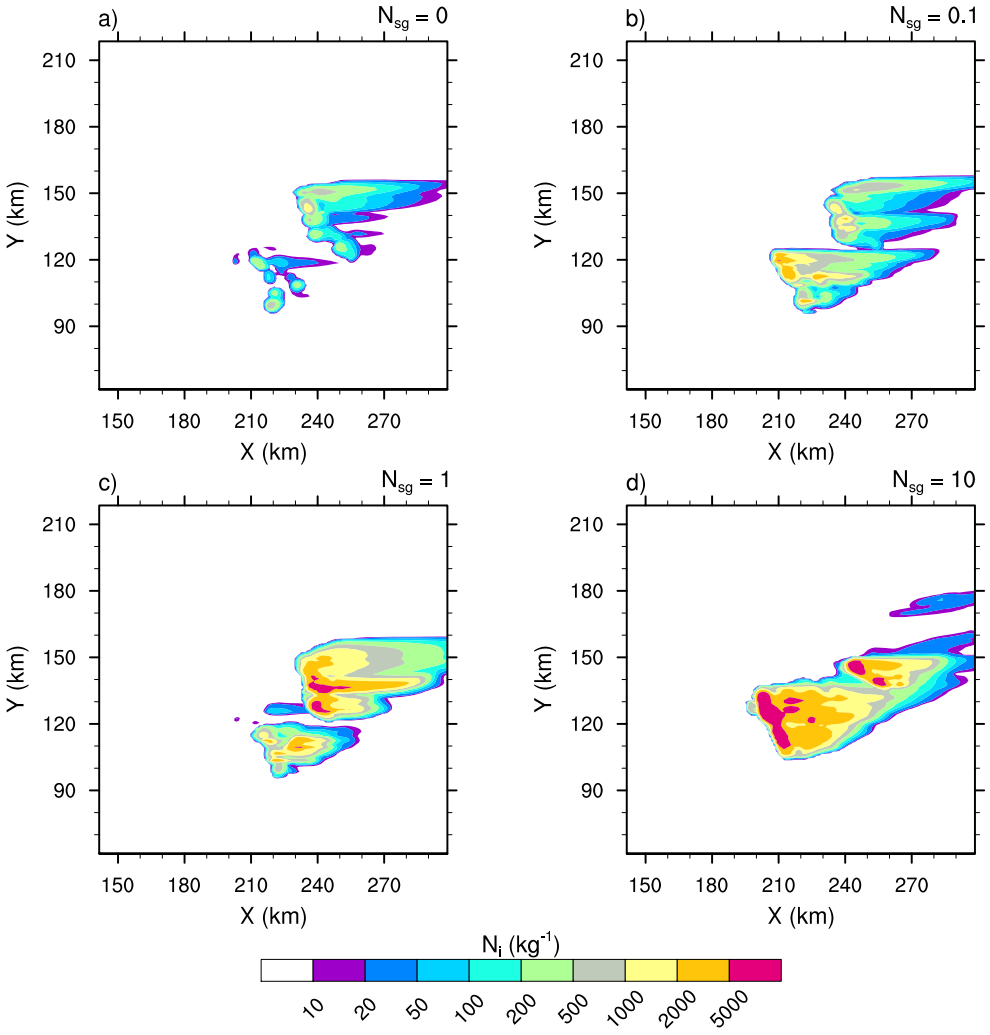


**Figure 6.** Number concentration of the cloud ice ($N_i$ in log scale) of the STERAO simulations at 15 km height, where a) to d) refer to cases with $\mathcal{N}_{sg}$=0.0, 0.1, 1.0 and 10.0 ice fragments per collision, respectively. The plots are for a fraction of the computational domain.

Geosci. Model Dev. Discuss., https://doi.org/10.5194/gmd-2017-287
Manuscript under review for journal Geosci. Model Dev.
Discussion started: 5 December 2017


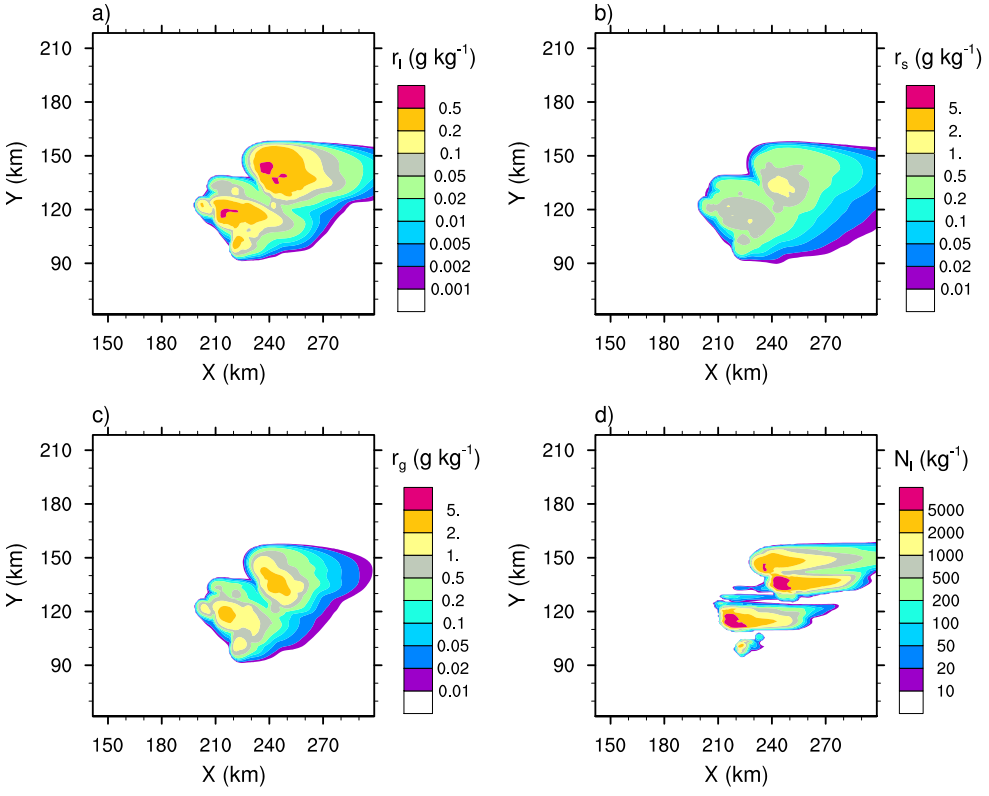


**Figure 7.** "RANDOM" case of the STERAO simulations showing the mixing ratios of a) the cloud ice ($r_i$), b) the snow-aggregates ($r_s$), and c) the graupel ($r_g$) at 12 km height. Plot d) refers to the number concentration of the cloud ice crystals ($N_i$) at 15 km height. The plots are for a fraction of the computational domain.

Geosci. Model Dev. Discuss., https://doi.org/10.5194/gmd-2017-287
Manuscript under review for journal Geosci. Model Dev.
Discussion started: 5 December 2017


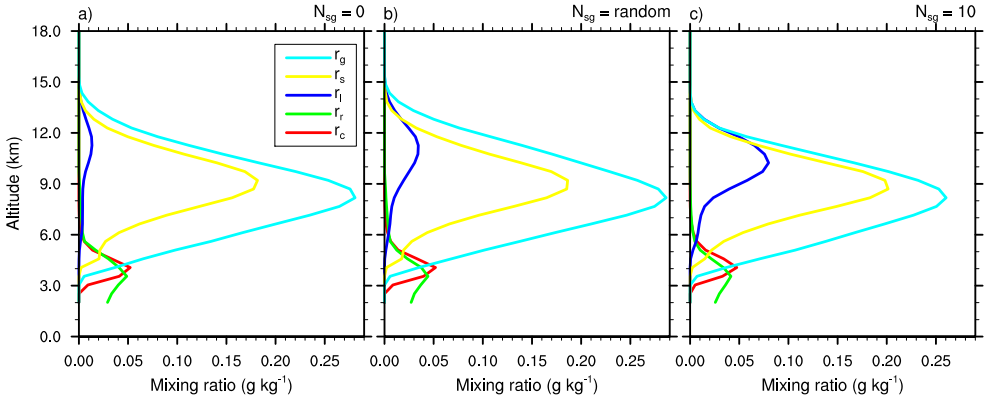


**Figure 8.** Mean profiles of condensate mixing ratios $r_c$, $r_r$, $r_i$, $r_s$ and $r_g$ ; in g kg$^{-1}$) of the STERAO simulations corresponding to a) the $\mathcal{N}_{sg}$=0.0 case, b) the "RANDOM" case and c) the case with $\mathcal{N}_{sg}$ = 10.0.

Geosci. Model Dev. Discuss., https://doi.org/10.5194/gmd-2017-287
Manuscript under review for journal Geosci. Model Dev.
Discussion started: 5 December 2017


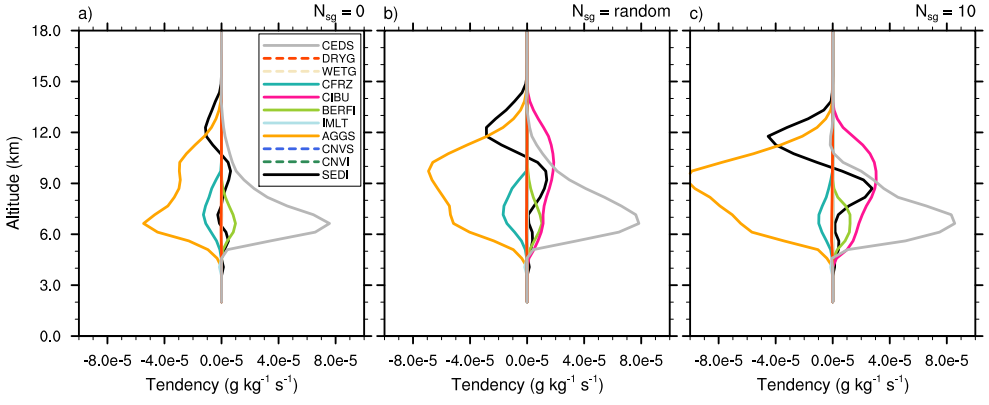


**Figure 9.** Mean microphysics profiles of cloud ice mixing ratio tendencies of the STERAO simulations corresponding to a) the $\mathcal{N}_{sg}$ = 0.0 (no CIBU) case, b) the "RANDOM" case and c) the case with $\mathcal{N}_{sg}$ = 10.0. The dashed lines are associated with processes having no significant impact on these budgets.

Geosci. Model Dev. Discuss., https://doi.org/10.5194/gmd-2017-287
Manuscript under review for journal Geosci. Model Dev.
Discussion started: 5 December 2017


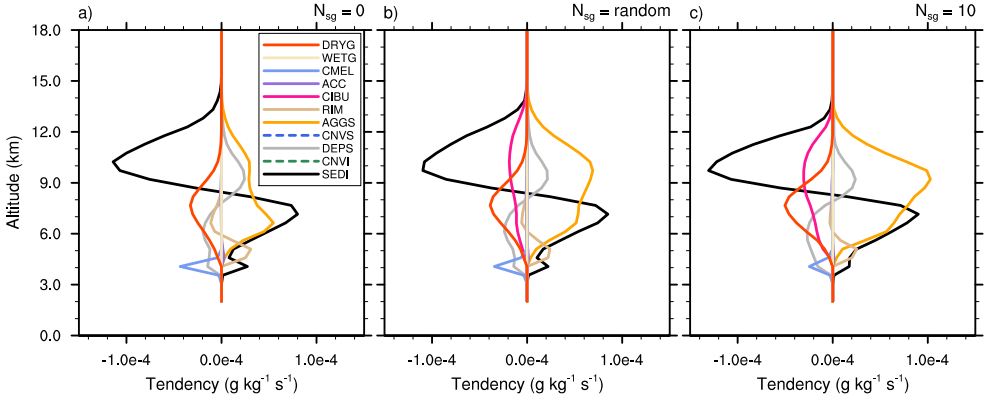


**Figure 10.** Same as Fig. 9 but for snow-aggregates.

Geosci. Model Dev. Discuss., https://doi.org/10.5194/gmd-2017-287
Manuscript under review for journal Geosci. Model Dev.
Discussion started: 5 December 2017


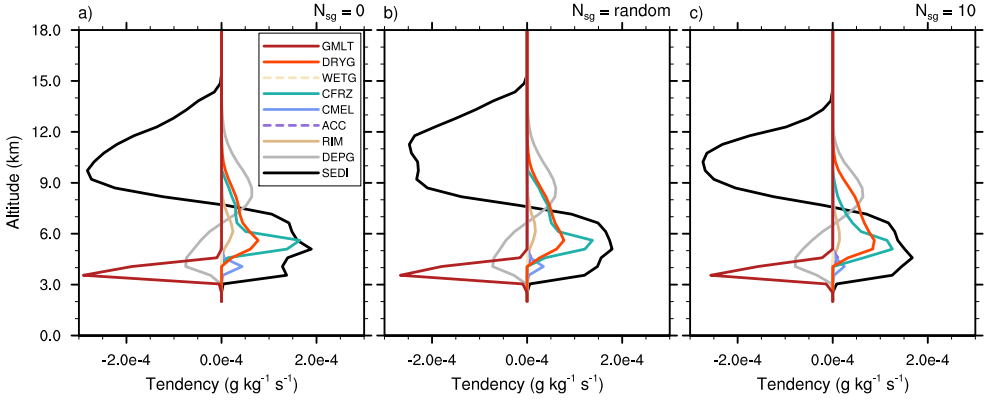


**Figure 11.** Same as Fig. 9 but for graupel.

Geosci. Model Dev. Discuss., https://doi.org/10.5194/gmd-2017-287
Manuscript under review for journal Geosci. Model Dev.
Discussion started: 5 December 2017


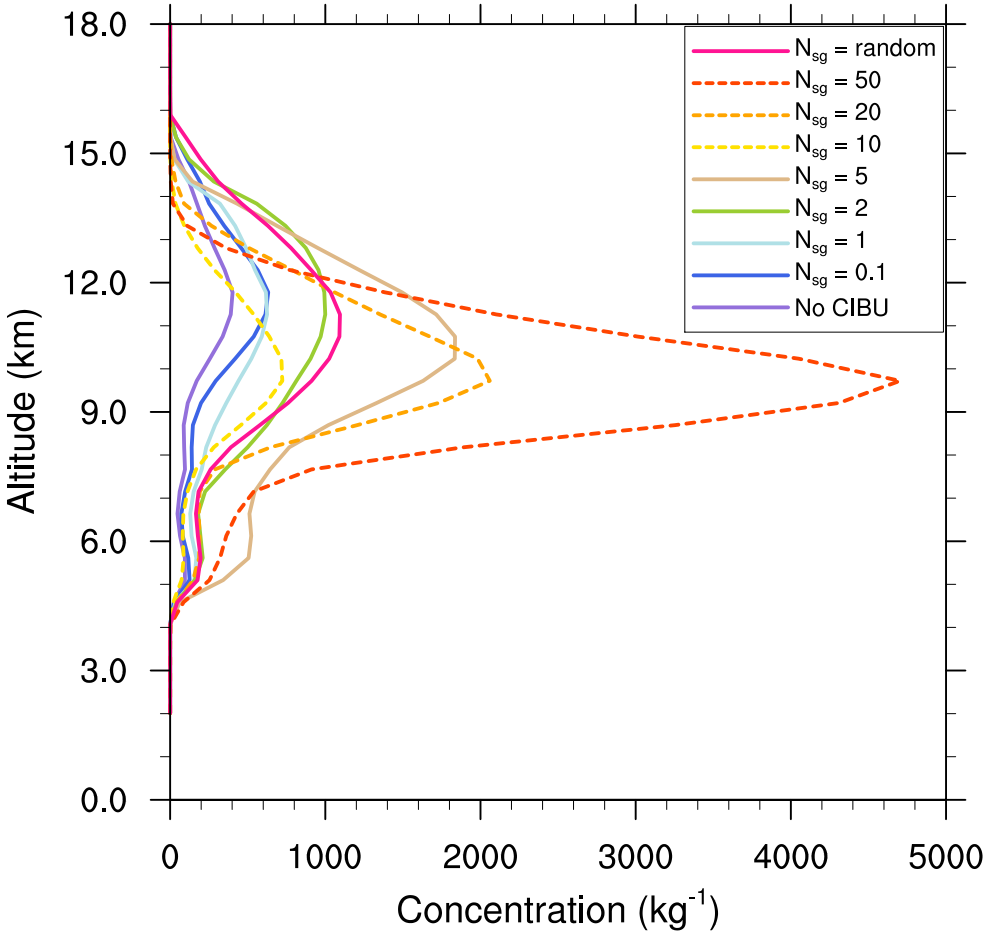


**Figure 12.** Mean profiles of the cloud ice crystal concentrations $N_i$ (g kg$^{-1}$) of the STERAO simulations corresponding to different values of $\mathcal{N}_{sg}$ (see the legend for details). The profiles drawn with a dashed line have been divided by 10 to fit into the plot.

Geosci. Model Dev. Discuss., https://doi.org/10.5194/gmd-2017-287
Manuscript under review for journal Geosci. Model Dev.
Discussion started: 5 December 2017


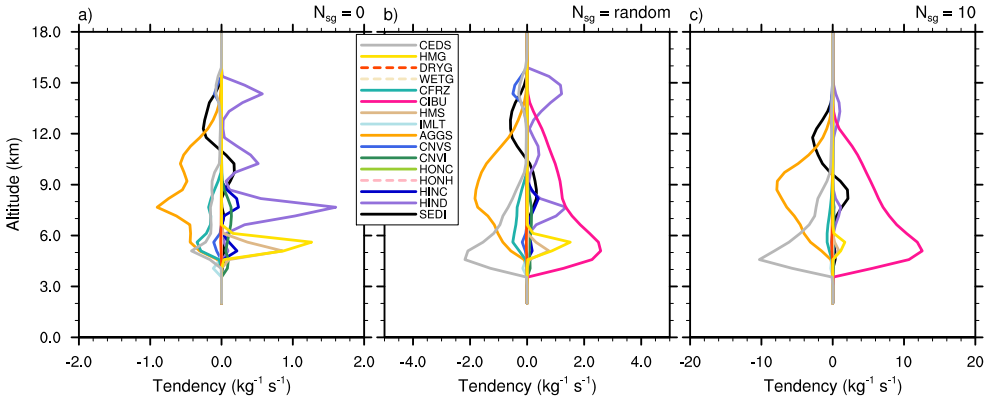


**Figure 13.** Mean microphysics profiles of the cloud ice crystal concentration tendencies of the STERAO simulations corresponding to a) the $\mathcal{N}_{sg}$ = 0.0 (no CIBU) case, b) the "RANDOM" case and c) the case with $\mathcal{N}_{sg}$ = 10.0 (Note that the horizontal scale increases from a) to c)). The dashed lines of the list box are associated with processes having no significant impact on these budgets.

Geosci. Model Dev. Discuss., https://doi.org/10.5194/gmd-2017-287
Manuscript under review for journal Geosci. Model Dev.
Discussion started: 5 December 2017


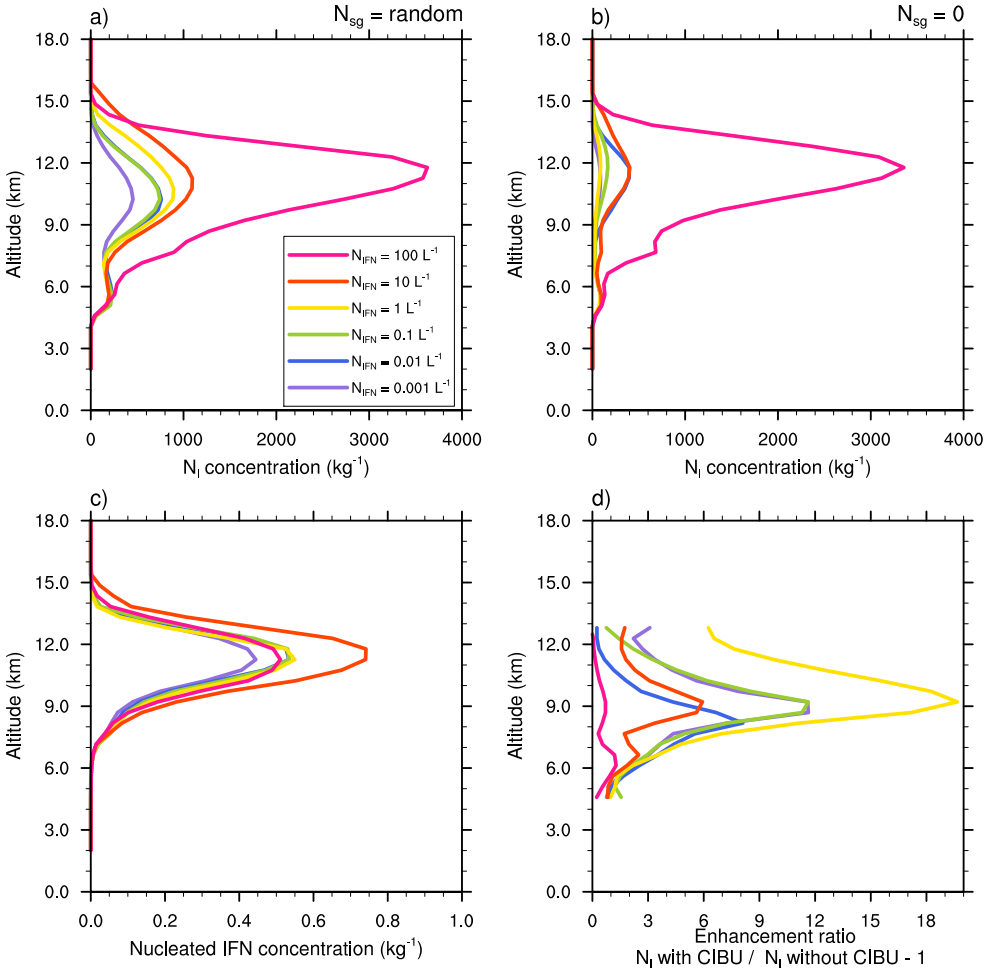


**Figure 14.** Mean profiles of cloud ice crystal concentration for 6 decades of initial IFN concentrations from 100 $dm^{-3}$ to 0.001 $dm^{-3}$ of the STERAO simulations corresponding to a) the CIBU simulation and "RANDOM" case and b) the non-CIBU simulation. The mean profiles of the nucleated IFN concentrations are plotted in c) after rescaling to fit the [0.0-1.0] range. The rough estimate of CIBU enhancement factor of Ni is plotted in d) as a function of the initial IFN concentrations.